

SCIENTIFIC REPORTS



OPEN

Burkholderia cenocepacia and *Salmonella enterica* ArnT proteins that transfer 4-amino-4-deoxy-L-arabinose to lipopolysaccharide share membrane topology and functional amino acids

Received: 27 January 2015

Accepted: 01 May 2015

Published: 01 June 2015

Faviola Tavares-Carreón¹, Kinnari B. Patel² & Miguel A. Valvano^{1,2}

We recently demonstrated that incorporation of 4-amino-4-deoxy-L-arabinose (L-Ara₄N) to the lipid A moiety of lipopolysaccharide (LPS) is required for transport of LPS to the outer membrane and viability of the Gram-negative bacterium *Burkholderia cenocepacia*. ArnT is a membrane protein catalyzing the transfer of L-Ara₄N to the LPS molecule at the periplasmic face of the inner membrane, but its topology and mechanism of action are not well characterized. Here, we elucidate the topology of ArnT and identify key amino acids that likely contribute to its enzymatic function. PEGylation assays using a cysteineless version of ArnT support a model of 13 transmembrane helices and a large C-terminal region exposed to the periplasm. The same topological configuration is proposed for the *Salmonella enterica* serovar Typhimurium ArnT. Four highly conserved periplasmic residues in *B. cenocepacia* ArnT, tyrosine-43, lysine-69, arginine-254 and glutamic acid-493, were required for activity. Tyrosine-43 and lysine-69 span two highly conserved motifs, ⁴²RYA⁴⁴ and ⁶⁶YFEKP⁷⁰, that are found in ArnT homologues from other species. The same residues in *S. enterica* ArnT are also needed for function. We propose these aromatic and charged amino acids participate in either undecaprenyl phosphate-L-Ara₄N substrate recognition or transfer of L-Ara₄N to the LPS.

The Gram-negative opportunistic bacterium *Burkholderia cenocepacia* causes serious lung infections in patients with cystic fibrosis^{1,2}. *B. cenocepacia* is difficult to treat because of its extraordinarily high intrinsic resistance to virtually all clinically useful antibiotics including antimicrobial peptides such as the polymyxins³⁻⁵. Intrinsic resistance of *B. cenocepacia* depends in part on its lipopolysaccharide (LPS)⁶⁻⁸. *B. cenocepacia* can modify its LPS lipid A moiety by incorporating 4-amino-4-deoxy-L-arabinose (L-Ara₄N). The LPS inner core oligosaccharide contains a side branch D-glycero-D-talo-octo-2-ulosonic acid, which is also modified by L-Ara₄N^{9,10}. These modifications neutralize negative charges in the LPS molecule, inhibiting binding of cationic molecules¹¹. Remarkably, L-Ara₄N modification in *B. cenocepacia* is essential for bacterial viability¹², since it is required for LPS export to the outer membrane¹³, and for high resistance to polymyxin B (PmB) at concentrations reaching milligram range^{4,7,8,13,14}.

¹Centre for Human Immunology, Department of Microbiology and Immunology, University of Western Ontario, London, Ontario, N6A 5C1, Canada. ²Centre for Infection and Immunity, Queen's University Belfast, Belfast, BT9 7AE, United Kingdom. Correspondence and requests for materials should be addressed to M.A.V. (email: m.valvano@qub.ac.uk)

L-Ara4N biosynthesis occurs in the cytoplasm by the enzymes AraABCD. This process converts UDP-glucuronic acid into L-Ara4N linked to undecaprenyl phosphate¹⁵. Undecaprenyl phosphate-L-Ara4N is translocated across the inner membrane by the heterodimer ArnE-ArnF flippase¹⁶ and finally ArnT transfers L-Ara4N to the lipid A in a reaction occurring at the periplasmic face of the inner membrane¹⁷. Hamad *et al.*¹³ postulated that *B. cenocepacia* ArnT also transfers L-Ara4N to the inner core D-glycero-D-talo-octo-2-ulopyranosic acid, but this was not directly demonstrated. Because the transfer of L-Ara4N to the LPS is essential for *B. cenocepacia* viability^{12,13}, Δ arnT mutants are only viable if a suppressor mutation occurs in the *lptG* gene encoding a component of the LPS transport pathway, which allows export of unmodified LPS¹³.

Lipid A modifications requiring ArnT family proteins have been reported in *Escherichia coli*, *Salmonella enterica* serovar Typhimurium and *Pseudomonas aeruginosa* where LPS is modified with L-Ara4N^{18,19}, and in *Francisella novicida* and two *Bordetella* species (*B. bronchiseptica* and *B. pertussis*) where LPS is modified with galactosamine and glucosamine, respectively^{20–22}. Since LPS modifications contribute to pathogenicity and innate immunity evasion, ArnT can be considered a virulence factor in these bacteria.

ArnT is an integral membrane protein; its topology was partially characterized in *S. enterica*²³, but little is known on functional regions and enzyme mechanism. Elucidating the topology of ArnT is critical to understand its function and developing molecules targeting L-Ara4N modification of LPS, which would abolish intrinsic bacterial resistance to antimicrobial peptides. In this study, we characterize the topology of *B. cenocepacia* and *S. enterica* ArnT. Both proteins show very similar topology, suggesting the topological arrangement in other proteins of the ArnT family is likely conserved. We propose ArnT proteins consist of thirteen transmembrane domains with two large periplasmic loops and a C-terminal segment that is exposed to the periplasm. We also identify four highly conserved periplasmic amino acids that are presumably involved in ArnT function.

Results

ArnT is a membrane protein with 13 predicted transmembrane helices. To facilitate immunodetection while exploring the ArnT topology we constructed a recombinant protein carrying a C-terminal FLAG-10xHis tag. ArnT_{FLAG-10xHis} was expressed under the control of a rhamnose-inducible promoter in the Δ arnT-arnBC⁺lptG_{D31H} suppressor strain (herein Δ arnT)¹³. This *B. cenocepacia* strain is viable but highly sensitive to PmB due to lack of L-Ara4N in the LPS¹³. In the presence of rhamnose, ArnT_{FLAG-10xHis} restored Δ arnT PmB resistance to parental levels (Supplementary Figure S1A online), and was detected by immunoblot as a polypeptide with an apparent mass of 63 kDa, in agreement with its predicted mass of 66.3 kDa (Supplementary Figure S1B online). These experiments demonstrate that the FLAG-10xHis tag does not affect ArnT function and membrane localization.

Earlier work suggested that *S. enterica* and *E. coli* ArnT proteins contain 12 predicted transmembrane helices and that the C-terminus is in the cytosolic compartment^{17,23}. However, an *in silico* model of *B. cenocepacia* ArnT topology with PolyPhobius predicted 13 transmembrane helices and a large C-terminus exposed to the periplasmic space in both *S. enterica* and *E. coli* ArnT proteins (Fig. 1). To provide experimental evidence for the predicted ArnT transmembrane topology we used the substituted cysteine accessibility method with methoxypolyethylene glycol maleimide (PEG-mal) labeling^{24,25}. PEG-mal is a maleimide conjugate that modifies cysteines but cannot cross membranes. Reaction of a cysteine with PEG-mal results in a mass addition of ~5 kDa to the protein, which appears as a band shift by immunoblotting. PEG-mal modification using EDTA-permeabilized whole cells indicates that the cysteine has a periplasmic orientation, while PEG-mal modification under denaturing conditions (presence of SDS) suggests that the cysteine is within a transmembrane helix or faces the cytoplasm. *B. cenocepacia* ArnT_{FLAG-10xHis} has two cysteine residues at positions 154 and 176, which were replaced by alanine to generate a cysteineless derivative (ArnT_{Cysless}). ArnT_{Cysless} and the single cysteine replacement derivatives (ArnT_{C154A} and ArnT_{C176A}) restored PmB resistance in Δ arnT at similar levels as the wild type strain (Fig. 2A), demonstrating that the native cysteines are dispensable for ArnT function. Using PEG-mal labeling, we observed that ArnT_{C154A} and ArnT_{C176A} were only PEGylated in detergent (2% SDS), while ArnT_{Cysless} was not PEGylated under any condition (Fig. 2B). These results suggest that Cys-154 and Cys-176 are buried in transmembrane helices, as predicted by the *in silico* model (Fig. 1). Cell membrane integrity in these experiments was confirmed by co-expressing ArnT_{C154} and ArnT_{C176} with HA-SoxY, a cytoplasmic protein that is highly PEGylated²⁴. Immunoblotting using anti-HA antibodies shows that HA-SoxY was only PEGylated under denaturing conditions (Fig. 2B), demonstrating that the bacterial membranes remained intact.

To confirm whether Cys-154 and Cys-176 are indeed buried, PEGylation was performed in the presence or absence of N-ethylmaleimide (NEM). NEM is a small sulfhydryl-reactive molecule that crosses membranes, but cannot react with cysteines embedded within the membrane bilayer²⁶. As a control, we used a phenylalanine-247 cysteine replacement mutant, since this residue is predicted to reside in the periplasmic side. PEGylation of the resulting protein was examined in samples pretreated with or without NEM, and also with or without SDS. This experiment showed that ArnT_{F247C} could be PEGylated in the absence of NEM (Fig. 2C), demonstrating a periplasmic orientation for this residue. In contrast, ArnT_{C154A} and ArnT_{C176A} were PEGylated despite treatment with NEM, demonstrating that the single cysteine remaining in each protein (Cys-176 in ArnT_{C154A} and Cys-154 in ArnT_{C176A}) is inaccessible to NEM modification (Fig. 2D), as would be expected if these residues are buried in the membrane bilayer.

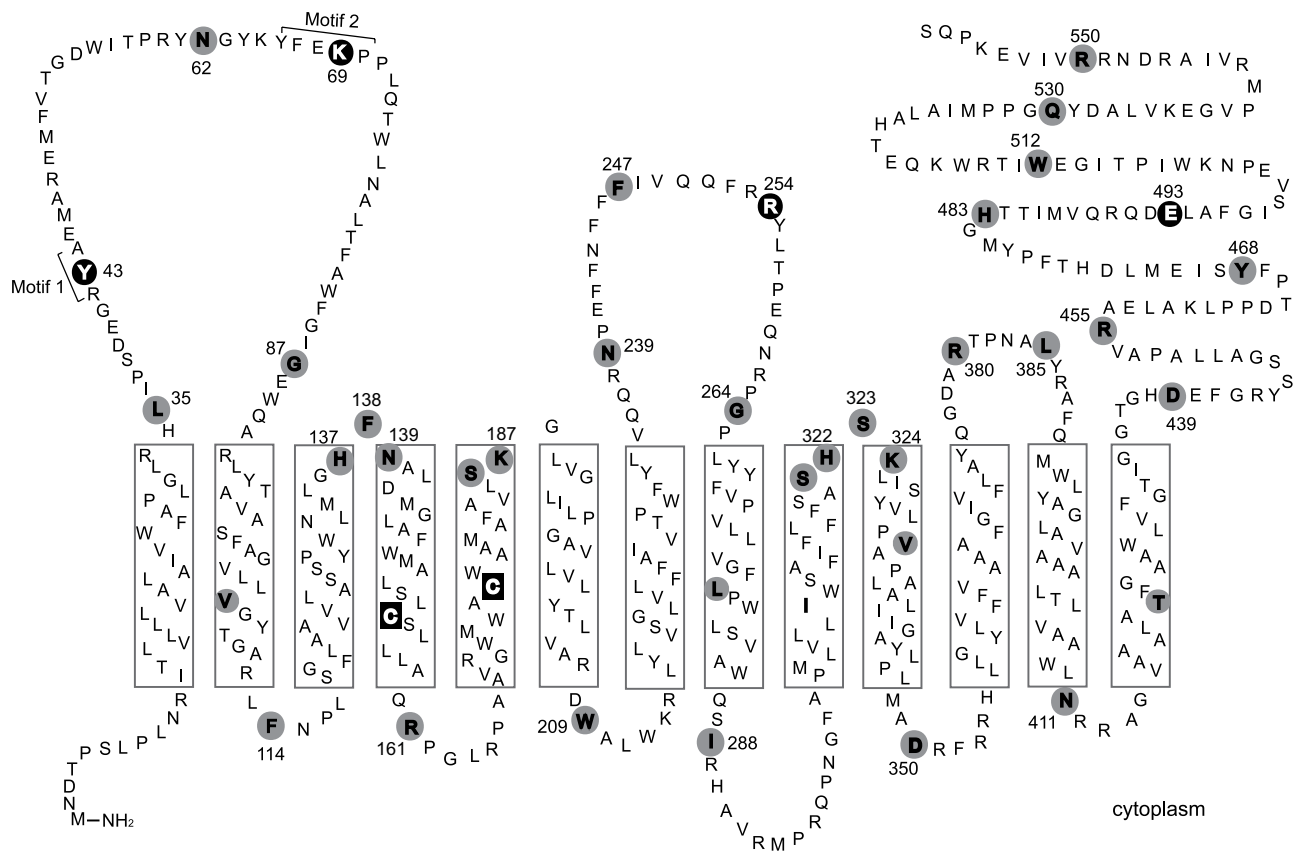


Figure 1. ArnT topological model. The model was derived using PolyPhobius and displayed with TMRPres2D. The ArnT C-terminus is oriented towards the periplasm and the protein has 13 predicted transmembrane helices, indicated by rectangles. The residues replaced by cysteine are shown in gray circles. Functional residues are indicated by black circle. The endogenous cysteines of ArnT are shown in black squares.

These results support the conclusion that the native cysteine residues in ArnT are in a transmembrane helix, as predicted by the *in silico* topological model.

More experimental evidence for the predicted ArnT topology was obtained by introducing 38 novel cysteine replacements at various positions of ArnT_{Cysless}. As before, mutant proteins were analyzed by immunoblotting to confirm that the cysteine substitution did not affect protein stability and membrane location (Supplementary Figure S2 online). Also, the ArnT cysteine replacements restored PmB resistance in Δ arnT to wild type levels. We then analyzed the topology of amino acids predicted to reside in transmembrane segments. Cysteine residues replacing valine-106, leucine-278, valine-332, and threonine-422 resulted in ArnT proteins that could only be PEGylated in SDS irrespective of NEM pretreatment (Fig. 2D), indicating that these amino acids are embedded in the membrane bilayer, as predicted by the *in silico* model.

Next, we examined cysteine replacements in leucine-35, tyrosine-43, asparagine-62, lysine-69, glycine-87, asparagine-239, phenylalanine-247, arginine-254, glycine-264, arginine-380 and leucine-385. All of the resulting proteins could be PEGylated under non-denaturing conditions in whole cells, indicating that these residues are exposed to the periplasm (Fig. 3A). In contrast, proteins with cysteine replacements in residues located in predicted periplasmic hinges such as histidine-137, asparagine-139, serine-186, lysine-187, serine-321, histidine-322 and lysine-324, only reacted with PEG-mal upon SDS treatment (Fig. 3B), suggesting these residues are most likely embedded in the bilayer. However, ArnT_{F138C} and ArnT_{S323C} were PEGylated under non-denaturing conditions, indicating that these residues are exposed to the periplasm (Fig. 3B). To confirm this assertion we labeled total membrane preparations with and without NEM pretreatment to differentiate between solvent exposed and lipid bilayer buried residues. Membrane preparations containing proteins with cysteine replacements in histidine-137, asparagine-139, serine-186, lysine-187, serine-321, histidine-322, and lysine-324 were PEGylated in the presence of NEM, indicating that these residues are not solvent-exposed (Fig. 3C); while ArnT_{F138C} and ArnT_{S323C} only were PEGylated in the absence of NEM (Fig. 3C), demonstrating a periplasmic orientation for these residues. The intensity of the PEGylated band varied in some cases such as in ArnT_{L35C}

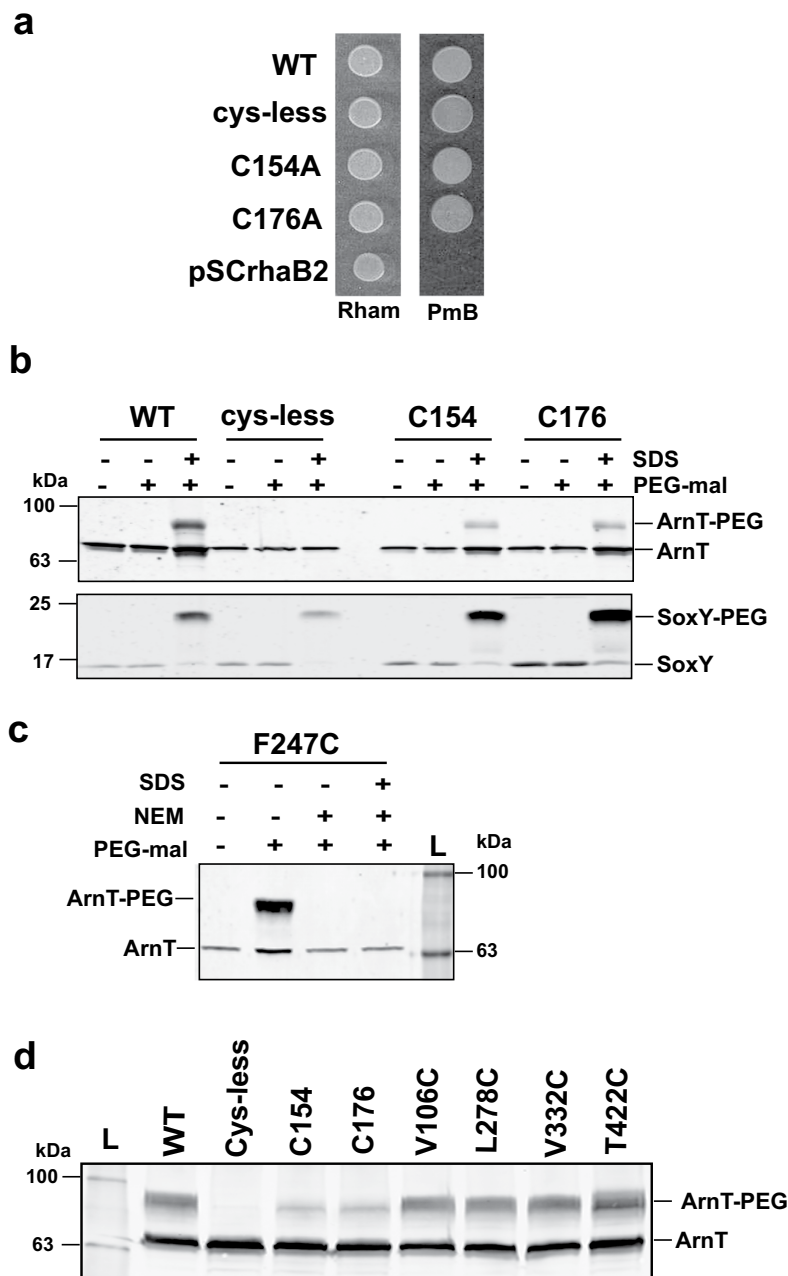


Figure 2. Native cysteines in ArnT are located in transmembrane segments. (a) Cys-less ArnT protein remains functional. Complementation of the Δ arnT-arnBC⁺ suppressor strain transformed with pSCrhaB2 encoding ArnT_{Cys-less}, ArnT_{C154A}, and ArnT_{C176A}. Cells expressing ArnT_{FLAG-10xHis} and the vector pSCrhaB2 were used as controls. The transformants were spotted on LB supplemented with 0.4% of L-rhamnose (Rham) and 10 μ g ml⁻¹ PmB. (b) *E. coli* DH5 α containing a plasmid encoding SoxY was transformed with plasmids expressing ArnT_{Cys-less}, ArnT_{C154A} and ArnT_{C176A}. Bacteria were grown to mid-exponential phase and protein expression induced with 0.2% L-arabinose. Cells were harvested and resuspended in 0.3 ml of HEPES/MgCl₂ buffer. 0.1 ml of cell suspension was incubated with buffer alone or 1 mM PEG-mal with or without 2% SDS for 1h at room temperature. Reactions were quenched with 45 mM DTT, and proteins were separated by SDS-PAGE and transferred to nitrocellulose membrane. ArnT derivatives were detected with anti-FLAG and SoxY with anti-hemagglutinin serum. (c) For NEM blocking, cells were harvested and resuspended in 0.4 ml of HEPES/MgCl₂ buffer, then were incubated with 5 mM NEM for 30 min to block accessible sulfhydryl groups. The pellet was washed twice with 0.5 ml of ice-cold HEPES/MgCl₂ buffer and finally was PEGylated as indicated for panel b. (d) Cells were harvested and resuspended in 0.4 ml of HEPES/MgCl₂ buffer. 0.1 ml of the cell suspension was incubated with 5 mM NEM for 30 min, and then was treated with 1 mM PEG-mal and 2% SDS as indicated in panel B. The position of the molecular mass marker is indicated to the left, and the position of PEGylated and non-PEGylated protein to the right.

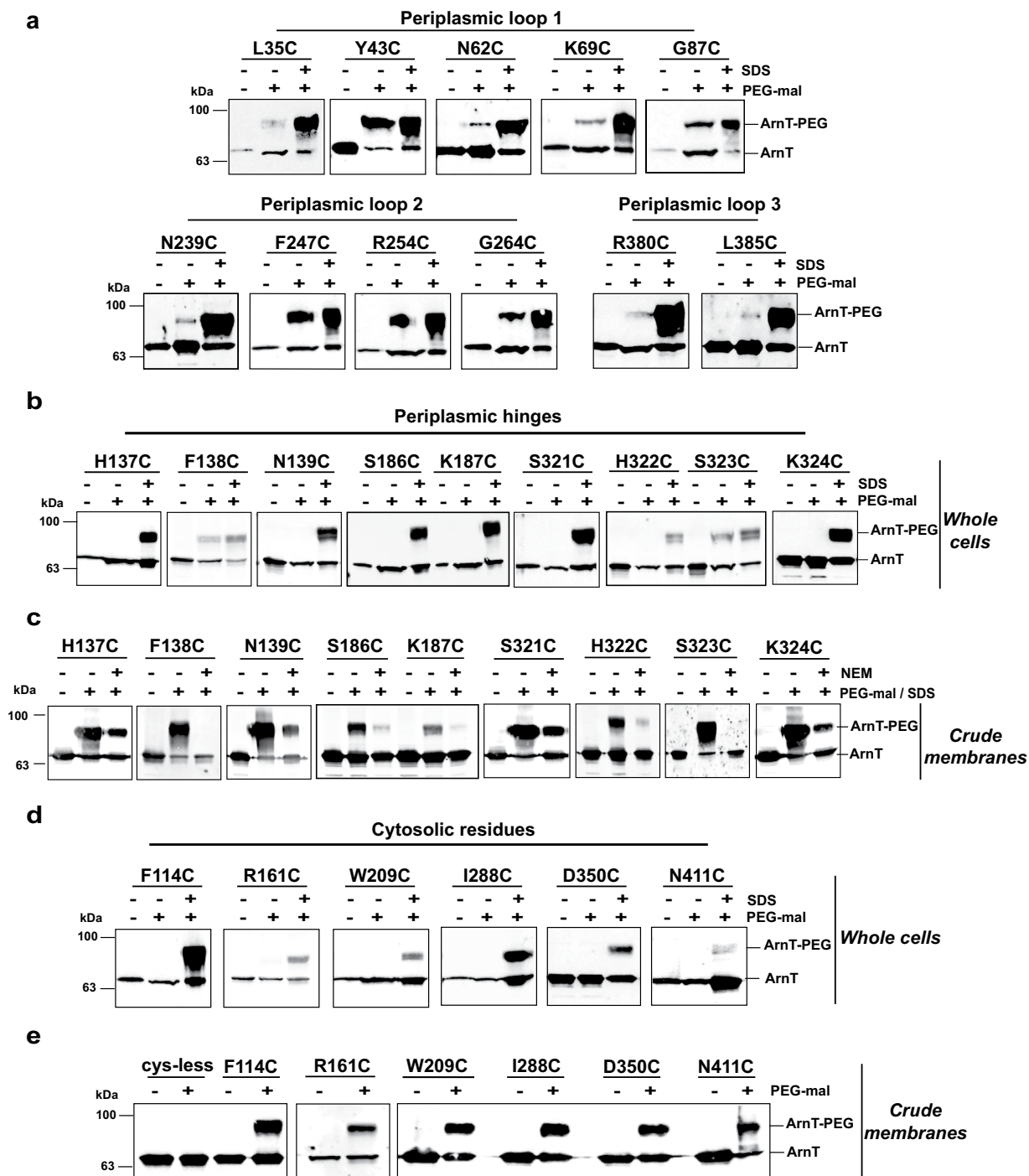


Figure 3. PEG-mal labeling of periplasmic and cytoplasmic ArnT amino acids. (a, b, and d) *E. coli* DH5 α carrying plasmids encoding ArnT cysteine replacements were grown to mid-exponential phase and protein expression induced with 0.2% L-arabinose. Cells were harvested and resuspended in 0.3 ml of HEPES/MgCl₂ buffer. 0.1 ml of cell suspension was incubated with buffer alone or 1 mM PEG-mal with or without 2% SDS for 1 h at room temperature. Reactions were quenched with 45 mM DTT, and proteins were separated by SDS-PAGE and transferred to nitrocellulose membranes, followed by immunoblot with anti-FLAG antibodies. (c) Crude membrane fractions were incubated with buffer alone or pre-treated with 5 mM NEM, after that membrane were incubated with 1 mM PEG-mal and 2% SDS for 1 h at room temperature. Reactions were quenched with 45 mM DTT. (e) Crude membrane fractions were isolated by ultracentrifugation and divided in two aliquots. One aliquot was incubated with buffer alone and the other with 1 mM PEG-mal. The reactions were quenched with 45 mM DTT and separated by SDS-PAGE. Immunoblot was probed with anti-FLAG antibody.

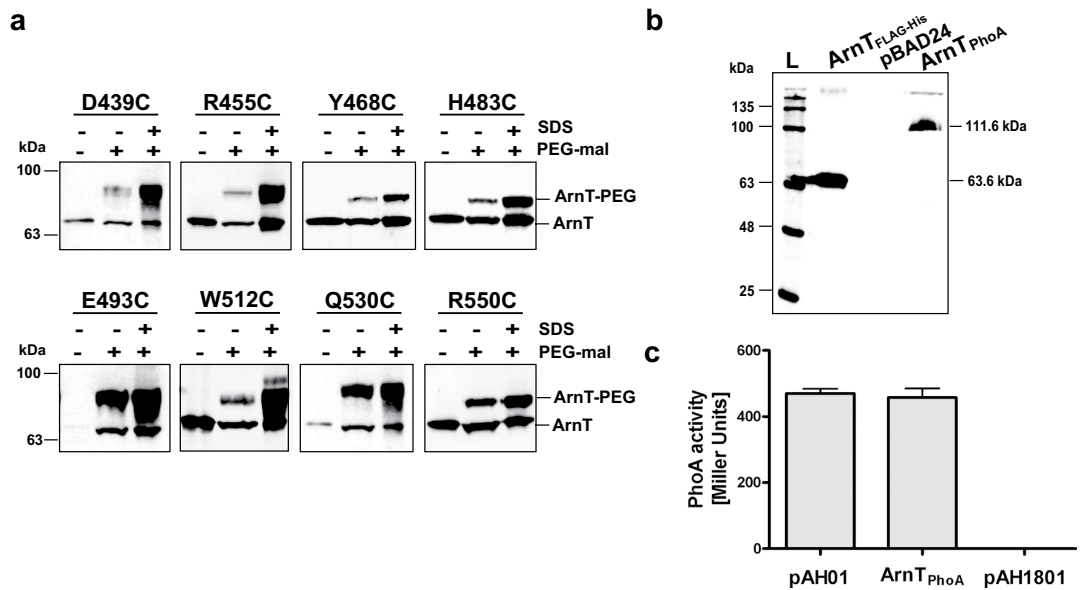


Figure 4. The ArnT C-terminus resides in the periplasmic space. (a) Whole cells from *E. coli* strain DH5 α carrying plasmids encoding cysteine-substitution of the C-terminal of ArnT were treated with buffer alone or 1 mM PEG-mal with or without 2% SDS for 1 h at room temperature and quenched with 45 mM DTT. Proteins were separated by SDS-PAGE and transferred to nitrocellulose membrane for blotting with anti-FLAG to detect ArnT. (b) Immunoblot of total membranes from *E. coli* CC118 cells expressing FLAG-ArnT_{PhoA} performed with anti-FLAG. L, BLUEye prestained protein ladder. (c) Quantification of PhoA activity in CC118 *E. coli* expressing FLAG-ArnT_{PhoA}. Cells were grown in LB and induced with 0.2% arabinose. Alkaline phosphatase activity was determined by measuring the rate of PNPP hydrolysis. pAH01 encodes FLAG-Wzx-K367-PhoA and pAH1801 encodes FLAG-Wzx-T242-PhoA, which were used as positive and negative controls, respectively³⁰. The values represent the mean \pm SE from three independent experiments.

or ArnT_{F138C} when examined by PEGylation of whole-cell preparations (Fig. 3A), and ArnT_{S186C} or ArnT_{K187C} when examined directly from membrane preparations (Fig. 3C). Because all the ArnT mutant proteins are equally expressed, we attributed reduced PEGylation to close proximity of the residue to the membrane bilayer border.

Cysteine replacements at phenylalanine-114, arginine-161, tryptophan-209, isoleucine-288, aspartic acid-350, and asparagine-411 resulted in proteins that were only PEGylated under prior denaturing conditions (Fig. 3D), suggesting they are on the cytosolic face of the membrane. These residues were also PEGylated in membrane preparations (Fig. 3E), as the conditions used for membrane disruption favor formation of inverted vesicles allowing exposure of cytoplasmic residues^{27,28}. Collectively, the experimental results support the *in silico* predicted ArnT topology.

The C-terminus of *B. cenocepacia* and *S. enterica* ArnT proteins resides in the periplasm. According to the *in silico* topological model, *B. cenocepacia* ArnT contains an extended C-terminal segment located towards the periplasm. To investigate the orientation of the 123-amino acid soluble C-terminal region of *B. cenocepacia* ArnT, we introduced eight cysteine replacements at aspartic acid-439, arginine-455, tyrosine-468, histidine-483, glutamic acid-493, tryptophan-512, glutamine-530, and arginine-550. The corresponding proteins were PEGylated in whole cells under non-denaturing conditions, demonstrating that these residues are exposed to the periplasm (Fig. 4A). We also constructed a version of ArnT that was C-terminally fused to PhoA (FLAG-ArnT_{PhoA}), a protein probing for periplasmic location²⁹, which was expressed in the *E. coli* Δ phoA CC118 strain. Immunoblotting of total membranes with the anti-FLAG antibody revealed a polypeptide band with an apparent mass of 111.6 kDa consistent with the FLAG-ArnT_{PhoA} predicted mass (Fig. 4B). The CC118 strain expressing the fusion protein produced 400 U of alkaline phosphatase activity (Fig. 4C), which was comparable to that of the positive control (CC118 expressing Wzx_{K367}-PhoA)³⁰. Together, these experiments strongly support the conclusion that the C-terminal region of *B. cenocepacia* ArnT is oriented towards the periplasm.

In a previous report²³, the C-terminal region of the *S. enterica* ArnT was assigned to the cytosol without experimental confirmation and despite that a periplasmic location was predicted *in silico*. ArnT_{Se} has eight native cysteine residues, two of which (C148 and C149) were predicted to be in the second periplasmic loop and the remaining six cysteines embedded in transmembrane segments²³. Therefore, we constructed a double replacement mutant, ArnT_{C148A-C149A}, which was used to further introduce novel cysteines in the C-terminal domain without making a complete Cys-less version of ArnT_{Se}. Novel

cysteines replaced glutamic acid-438, aspartic acid-469, arginine-506, and glutamine-544 residues. Mutant proteins and parental ArnT_{se} were detectable by immunoblotting (Fig. 5A). PEGylation was performed in whole cells with and without detergent. ArnT_{E438C}, ArnT_{D469C}, ArnT_{R506C} and ArnT_{Q544C} were PEGylated in non-denaturing conditions (Fig. 5B). Since all these residues were accessible to PEG-mal we concluded that they are exposed to the periplasmic face and not to the cytosolic space as previously proposed²³. As a control, the cytoplasmic HA-SoxY protein was only PEGylated under SDS treatment (Fig. 5B), ruling out loss of cell membrane integrity during whole cell PEGylation. SDS treatment also showed PEGylation of the ArnT_{se} derivatives under denaturing conditions (Fig. 5B, asterisk), as expected given that there were six remaining native cysteines in the protein. Importantly, the parental ArnT_{se} was not PEGylated in absence of SDS (Fig. 5B), indicating that cysteines 148 and 149 are not exposed to the second periplasmic loop, as it was reported²³.

Further, we investigated the location of the ArnT_{se} C-terminus by constructing a PhoA fusion (FLAG-ArnT_{se}-PhoA). Immunoblot of total membrane preparations reacted with anti-FLAG (Fig. 5C) identified a 110.5-kDa-polypeptide band as expected, indicating that ArnT_{se} is correctly fused to the PhoA protein and that is also in the membrane fraction. Lysates of strain CC118 expressing the fusion protein displayed 350 U of alkaline phosphatase activity (Fig. 5D), which was comparable to the activity of the positive control cell lysates from CC118 expressing Wzx_{K367}-PhoA³⁰. Therefore, the ArnT_{se} C-terminal domain is exposed towards the periplasm, as in ArnT_{Bc}.

Identification of functional amino acids in ArnT. We examined the functionality of ArnT_{Bc} cysteine replacement mutants by determining their ability to restore PmB resistance when expressed in the *B. cenocepacia* Δ arnT *lptG* suppressor mutant (Supplementary Table S1 online). Only proteins with replacements at tyrosine-43, lysine-69, arginine-254, and glutamic acid-493 residues, all of which are exposed to the periplasmic space (Fig. 1), failed to complement PmB resistance. Multiple sequence alignment revealed that tyrosine-43, lysine-69 (first periplasmic loop), arginine-254 (second periplasmic loop), and glutamic acid-493 (C-terminal segment) residues are highly conserved in ArnT proteins from different bacteria. Also, tyrosine-43 and lysine-69 residues are part of two distinct highly conserved motifs: ⁴²RYA⁴⁴ and ⁶⁶YFEKP⁷⁰ (Fig. 1 and Supplementary Figure S3A online), further suggesting that the identified residues could play a functional role.

Because loss of function in ArnT_{Y43C}, ArnT_{K69C}, ArnT_{R254C}, and ArnT_{E493C} could also reflect structural modifications imposed by the non-native cysteine residue, we constructed alanine replacements at the same positions. The alanine replacement mutant proteins expressed at wild type levels and they also appeared in the membrane fraction (Supplementary Figure S3B online). To investigate whether the alanine replacement alters the local conformation of the loop, each residue before alanine-43, -69, -254, and -493 in ArnT_{Y43A}, ArnT_{K69A}, ArnT_{R254A}, and ArnT_{E493A} proteins was replaced by cysteine. PEGylation assays using the resulting proteins with cysteine/alanine replacements (ArnT_{R42C-Y43A}, ArnT_{E68C-K69A}, ArnT_{R253C-R254A}, and ArnT_{D492C-E493A}) showed labeling of the neighboring cysteines under non-denaturing conditions (Supplementary Figure S3C online). Since the residues next to the alanine replacements are also accessible to PEG-mal, we conclude that it would unlikely that the alanine replacements cause dramatic changes in the local conformation of the protein at these sites.

To investigate the contribution of the mutated residues to ArnT activity we evaluated the PmB sensitivity of Δ arnT expressing the alanine replacement mutant proteins. The wild type strain producing LPS with L-Ara4N was extremely resistant to PmB with a minimal inhibitory concentration (MIC) greater than 1,024 μ g ml⁻¹, while the Δ arnT MIC was 0.064 μ g ml⁻¹ (16,000-fold difference)¹³. MICs for Δ arnT expressing ArnT_{K69R}, ArnT_{R254A} and ArnT_{E493A} ranged from 8,000-fold reduction relative to wild type, while Δ arnT expressing ArnT_{K69A} and ArnT_{Y43A} had the same MIC as Δ arnT (Table 1), indicating that these replacements affected ArnT activity. Because alanine is a small amino acid typically used in replacements to prevent structural changes in proteins, we surmise that tyrosine-43, lysine-69, arginine-254 and glutamic acid-493 are involved in ArnT function.

Lysine-69, arginine-254, and glutamic acid-493 are charged amino acids. To investigate whether the charge or the nature of the amino acid is important for ArnT function we replaced lysine-69 with arginine and glutamic acid, arginine-254 with lysine and glutamic acid, and glutamic acid-493 with aspartic acid and lysine. All mutant proteins were detectable in whole cells by immunoblotting (Supplementary Figure S3D online). Neither lysine-69 nor arginine-254 replaced with opposite or same-charge amino acids resulted in proteins that could restore PmB resistance at MIC values similar to the wild type strain (Table 1). In contrast, ArnT containing glutamic acid-493 replaced by aspartic acid restored PmB resistance in Δ arnT at 128 μ g ml⁻¹ (Table 1), while the opposite charge substitution, ArnT_{E493K}, led to a MIC of 0.064 μ g ml⁻¹, identical to that of Δ arnT. Together, these data suggest that tyrosine-43 and lysine-69 are needed for ArnT function, and also that positive and negative charges at position 254 and 493, respectively, are required for ArnT activity.

The effect of the amino acid replacement mutants on ArnT function was also evaluated by examining the lipid A structure using matrix-assisted laser desorption ionization-time of flight (MALDI-TOF) mass spectrometry in the negative ion mode. The mass spectrum from the wild-type sample showed the presence of L-Ara4N as indicated by the ion peaks corresponding to tetra-acylated lipid A with one L-Ara4N in the monophosphate (at *m/z* 1496.8) and diphosphate (at *m/z* 1577.5) forms and penta-acylated lipid with one and two L-Ara4N (at *m/z* 1804.6 and *m/z* 1935.5, respectively) (Fig. 6A), agreeing with the

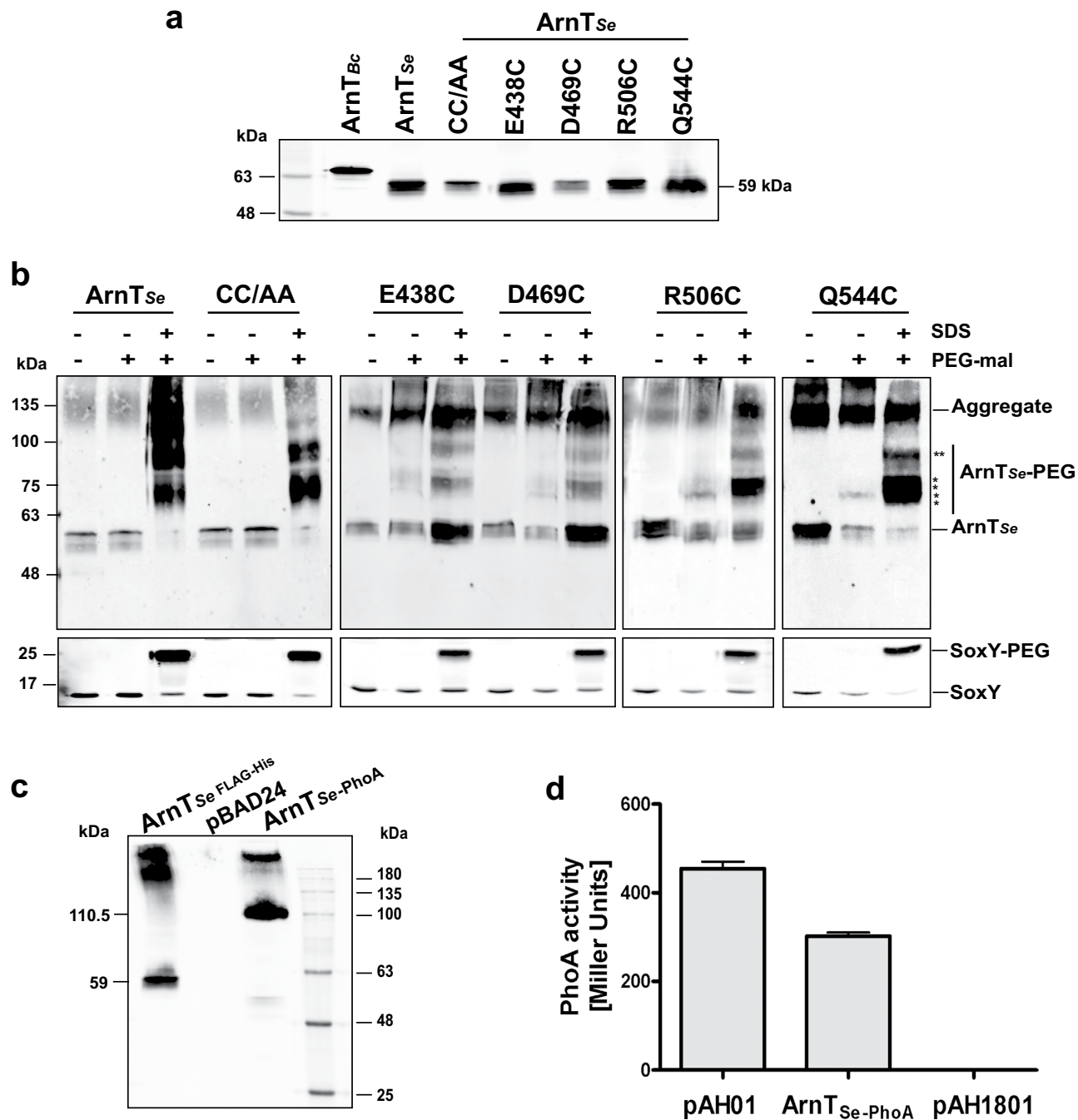


Figure 5. C-terminus of ArnT from *S. enterica* is located in the periplasm. (a) Immunoblot of total membranes isolated from *E. coli* DH5 α containing plasmids expressing ArnT_{Se} cysteine replacements. The proteins were separated by SDS-PAGE and immunoblotting was performed using anti-FLAG. ArnT_{Se}-FLAG-10xHis was used as control. C148A-C149A (CC/AA) was used as a template to generate the cysteine-substitution in the C-terminal of ArnT_{Se}. (b) PEGylated samples of ArnT_{Se} were prepared and analyzed as described in the legend to Fig. 2B. The positions of the molecular mass marker are indicated to the left. Asterisks indicate PEGylated ArnT_{Se} forms. ArnT_{Se} aggregates at the top of the western blots are attributed to the mild denaturing conditions. (c) Immunoblot of total membranes from *E. coli* CC118 cells expressing FLAG-ArnT_{Se}-PhoA performed with anti-FLAG. (d) Quantification of PhoA activity in CC118 *E. coli* expressing FLAG-ArnT_{Se}-PhoA. Cells were processed as described in the legend to Fig. 4C using the same positive and negative controls. The values represent the mean \pm SE from three independent experiments.

Residue	MIC ($\mu\text{g ml}^{-1}$)	Fold difference	Presence of L-Ara4N in lipid A
ArnT	>1,024	1	Yes
$\Delta\text{arnT-arnBC}^+$	0.064	16,000	No
ArnT _{Y43A}	0.064	16,000	No
ArnT _{K69A}	0.064	16,000	No
ArnT _{K69R}	0.125	8,192	Yes
ArnT _{K69E}	0.094	10,894	No
ArnT _{R254A}	0.125	8,192	Yes
ArnT _{R254K}	0.064	16,000	Yes
ArnT _{R254E}	0.064	16,000	No
ArnT _{E493A}	0.125	8,192	Yes
ArnT _{E493D}	128	8	Yes
ArnT _{E493K}	0.064	16,000	No

Table 1. PmB MIC values of cells expressing ArnT mutant proteins unable to complement the $\Delta\text{arnT-arnBC}^+$ $\text{lptG}_{\text{D31H}}$ (ΔarnT) suppressor mutant. MICs were determined by E-Test. The presence of L-Ara4N in the lipid A was determined by MS-MALDI-TOF using the negative ion mode, as described in Methods.

reported *B. cenocepacia* lipid A structure^{13,31}. As expected, these peaks were absent in the ΔarnT lipid A spectrum (Fig. 6B and Table 1). Mass spectrometry analysis of lipid A from ΔarnT expressing ArnT_{Y43A}, ArnT_{K69A}, ArnT_{K69E}, ArnT_{R254E} and ArnT_{E493K} did not reveal any peaks corresponding to glycoforms containing L-Ara4N (Table 1 and Supplementary Figure S4 online). Interestingly, L-Ara4N was present in $\Delta\text{arnT-arnBC}^+$ containing, ArnT_{K69R}, ArnT_{R254A}, ArnT_{R254K}, ArnT_{E493A}, and ArnT_{E493D} (Fig. 6C-G and Table 1). Because MALDI-TOF does not provide quantitative assessments, we interpreted the presence of L-Ara4N as a result of reduced but not abolished ArnT enzyme activity. This interpretation agrees with the hypersensitivity to PmB of the strain expressing these mutant proteins (Table 1), suggesting insufficient amount of lipid A modification to promote wild type levels of resistance to PmB. We therefore conclude that tyrosine-43, lysine-69, arginine-254 and glutamic acid-493 residues are important for ArnT function.

To better support these conclusions, we employed the conditional *B. cenocepacia* mutant $P_{\text{rha}}::\text{arnT}$, which only grows with rhamnose (permissive condition)¹³. Recombinant plasmids containing ArnT_{Bc} derivatives were introduced into $P_{\text{rha}}::\text{arnT}$ and the resulting transformants examined for viability without rhamnose in the medium. Recombinant plasmids expressing ArnT_{R254A}, ArnT_{R254K} and ArnT_{E493D} could rescue $P_{\text{rha}}::\text{arnT}$ growth without rhamnose (Supplementary Figure S5 online). In contrast, vector control and plasmids containing ArnT_{K69E}, ArnT_{R254E}, ArnT_{E493K} and ArnT_{E493A}, failed to rescue growth under the same condition. Bacteria containing ArnT_{K69A} and ArnT_{K69R} had moderate growth. These results agree with the lipid A structural analysis. Strains bearing ArnT_{R254A}, ArnT_{R254K} and ArnT_{E493D} had L-Ara4N in the LPS, and they could rescue viability in absence of rhamnose. Nevertheless, the MIC value from these strains is very similar to $\Delta\text{arnT-arnBC}^+$ except for the strains with ArnT_{E493D}, which behaves as the wild-type strain.

Together, these results indicate that ArnT with substitutions preserving the net charge of each residue were slightly functional, while substitutions reversing the charge caused loss of function. Therefore, the net charges in lysine-69 and arginine-254 are important for ArnT activity.

Tyrosine-36, lysine-62 and glutamic acid-478 are also important for *S. enterica* ArnT. An earlier report identified arginine-246 (corresponding arginine-254 of ArnT_{Bc}) as being functionally important for the *S. enterica* ArnT²³. We investigated whether ArnT_{Se} tyrosine-36, lysine-62, and glutamic acid-478 (corresponding to tyrosine-43, lysine-69, and glutamic acid-493 in ArnT_{Bc}, respectively) are also required for ArnT_{Se} function. However, the ArnT_{Se-FLAG-10xHis} fusion resulted in a protein that could not be detected by immunoblot. This could be due to structural constraints associated with a proline at the C-terminal end of the protein, which were resolved by replacing proline-547 by alanine without altering ArnT function³². Therefore, we constructed a P547A ArnT_{Se-FLAG-10xHis} protein and the corresponding alanine replacements in tyrosine-36, lysine-62, and glutamic acid-478. The recombinant proteins were tested for their ability to restore PmB resistance in an *E. coli* ΔarnT mutant. The complementation experiment indicated that these proteins could not confer PmB resistance, suggesting that the mutated residues are also important for ArnT activity in *S. enterica* (Fig. 7A); the stability of these proteins was not affected as shown by immunoblotting (Fig. 7B). Therefore, tyrosine-36, lysine-62 and glutamic acid-478 play a crucial role in the function of the ArnT_{Se}, demonstrating that the conserved amino acids in ArnT_{Bc} are also important in other ArnT family proteins.

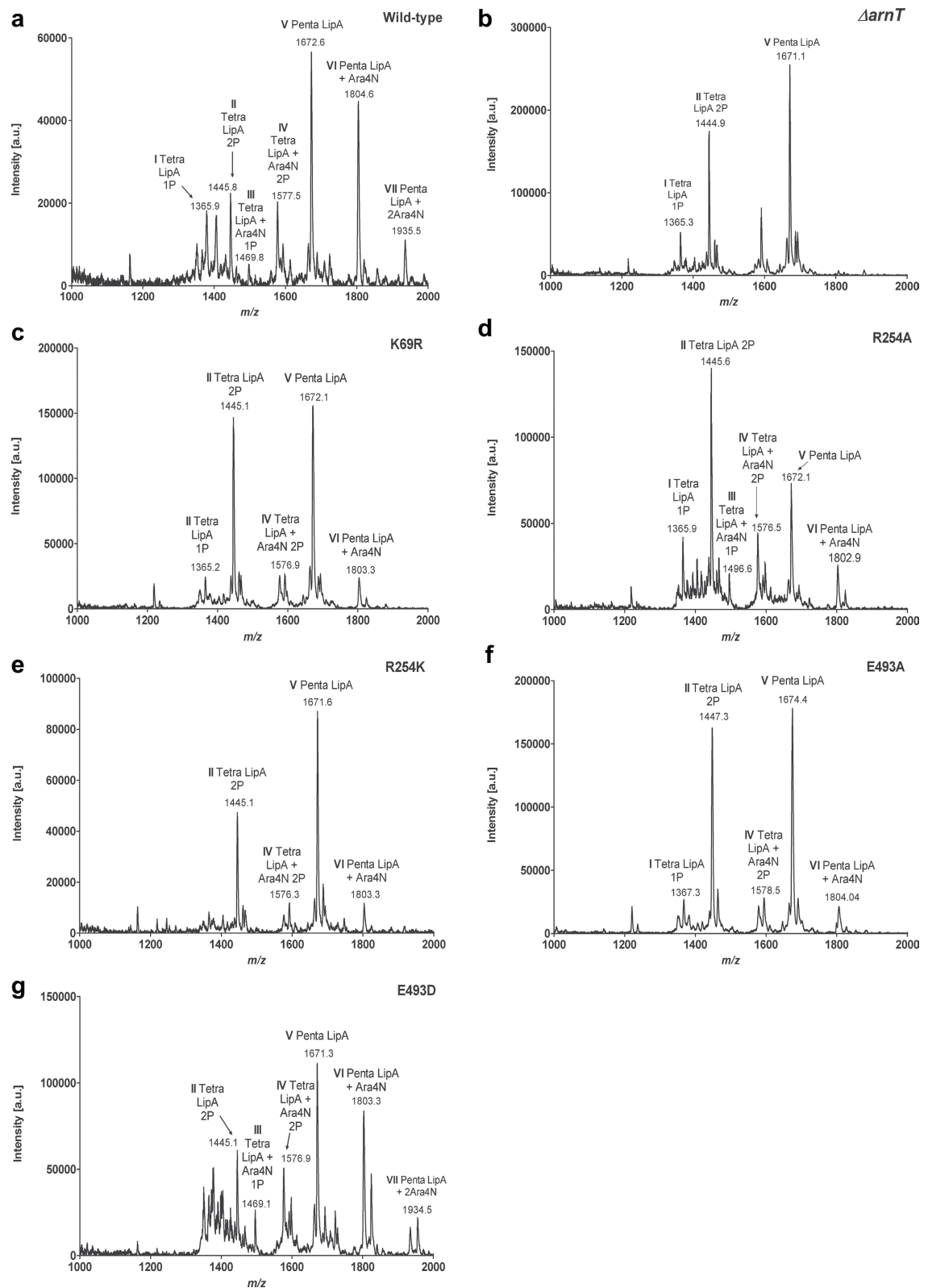


Figure 6. MALDI-TOF spectra of purified lipid A produced by *arnT* mutants. $\Delta arnT$ denotes strain MH55 ($\Delta arnT$ -*arnBC*⁺ *lptG*^S), which carries a *lptG* suppressor mutation (Table S1). Plasmids encoding *ArnT* proteins with various replacements are introduced into MH55 by triparental mating. The profiles represented were obtained using the negative ion mode. I-II Tetra-acylated lipid A with one or two phosphates molecules; III-IV, Tetra-acylated lipid A with one or two L-Ara4N molecules. V, Penta-acylated lipid A; VI-VII, Penta-acylated lipid A with one or two L-Ara4N molecules.

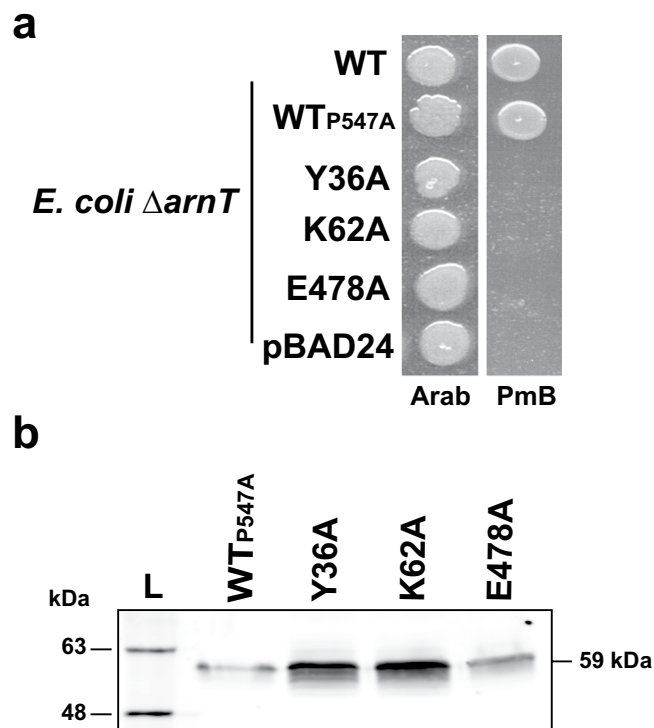


Figure 7. *S. enterica* ArnT shares the same functional residues than *B. cenocepacia* ArnT. (a) Complementation of *E. coli* Δ arnT with functional residues replaced with alanine from ArnT_{Se}. WT, ArnT_{P547A-FLAG-10xHis} as a positive control; pBAD24 as a negative control. Strains were spotted in LB plate with 0.2% arabinose (Arab) or 0.2% arabinose plus PmB 2.5 μ g/ml (PmB). (b) Total protein from cells expressing ArnT_{Se} derived proteins were separated by SDS-PAGE and detected with antibody anti-FLAG. L, molecular masses of protein standards.

Discussion

Glycosylation of the lipid A phosphate groups with L-Ara4N, catalyzed by ArnT, is a strategy commonly used by bacteria to overcome the action of antimicrobial peptides such as PmB³³. However, despite the growing number of ArnT homologs found in different bacteria to date very little is known on the mechanism of ArnT modification. We report in this work the membrane topology of *B. cenocepacia* and *S. enterica* ArnT proteins. Application of a topology prediction algorithm in combination with substituted cysteine scanning using PEGylation yielded an experimentally validated model for ArnT_{Bc} that suggests 13-transmembrane helices, two large periplasmic hydrophilic loops, and an extended C-terminus also located in the periplasm. Comparison of the *B. cenocepacia* ArnT model with an earlier model of ArnT from *S. enterica* reveals striking differences. Unlike ArnT_{Bc}, the proposed ArnT_{Se} model suggested four periplasmic loops and placed the C-terminal end towards the cytosol²³. Our PEGylation results do not support the earlier ArnT_{Se} model since two adjacent cysteines at positions 148 and 149, predicted to face the periplasm, were inaccessible to PEG-mal indicating they are buried in the membrane. In the previous model²³, the ArnT_{Se} C-terminus was also assigned a cytosolic location without any experimental validation and despite bioinformatic data suggesting the opposite. In contrast, our PEGylation data and a positive alkaline phosphatase ArnT-PhoA C-terminal fusion strongly support that the C-terminal segment of ArnT_{Se} is in the periplasm. We therefore conclude that *B. cenocepacia* and *S. enterica* ArnT proteins share similar topology, as expected for proteins of the same family performing the same function.

We also identified putative functional residues in ArnT_{Bc} that are highly conserved in ArnT proteins from different bacteria. These include tyrosine-43, lysine-69, and arginine-254. Furthermore, a negative charged amino acid is required at position 493 (glutamic acid in ArnT_{Bc}). All these putative functional residues reside on the periplasmic side of ArnT, as expected for an enzyme using substrates only available in the periplasm^{15,17}. We propose that these residues may participate either in catalysis or binding of the undecaprenyl-L-Ara4N donor substrate. Tyrosine-43 and lysine-69 residues are within two highly conserved motifs in all ArnT family members: ⁴²RYA⁴⁴ and ⁶⁶YFEKP⁷⁰. The conservation of these motifs within the first periplasmic loop of ArnT_{Bc} suggest not only that they are functionally relevant but more importantly, that the members of ArnT family share similar features. Further, replacing tyrosine-43 of the RYA motif by alanine or inverting the polarity of the lysine-69 resulted in a nonfunctional protein. It is possible that the first periplasmic loop containing two highly conserved motifs could define a putative catalytic reaction center conserved in all ArnT proteins. Mutagenesis of the arginine-254 residue residing

on the second periplasmic loop resulted in a protein with poor enzymatic activity. Agreeing with this conclusion, an arginine from ArnT_{Se} corresponding to ArnT_{Bc} arginine-254 was also reported to be important for the activity of this enzyme²³. Our data also suggest that the ArnT_{Se} second periplasmic loop, between amino acids 234 and 256, is required for function, as well as a C-terminal glutamic acid-493. Replacing this residue by aspartic acid, to maintain the same charge, resulted in a protein retaining the ability to incorporate L-Ara4N to lipid A and supports the notion that the ArnT C-terminus is also involved in the overall activity of this enzyme. However, our assignment of the functional residues has to remain tentative until validation by further biochemical investigations using purified protein, substrates, and acceptor molecules.

The mechanism of transfer of L-Ara4N to LPS remains to be elucidated. Superficially, ArnT proteins are analogous to O-antigen ligases and oligosaccharyl transferases. These proteins perform the enzymatic reaction on the periplasmic side of the membrane, and involve a metal ion-independent inverting glycosyltransfer reaction using undecaprenyl-bisphosphate-linked saccharide precursors³⁴. In contrast, bacteriophage-encoded glucosyltransferase proteins, which are responsible for the periplasmic transfer of glucose to the LPS O antigen moiety^{35,36}, utilize a lipid phosphate-activated glucosyl residue (Und-P-glucose)³⁷. ArnT proteins also utilize undecaprenyl-phosphate-linked saccharides, and the reaction occurs at the periplasmic site of the membrane¹⁷. Further, there is an inversion of the stereochemistry in the reaction since the substrate is Und-P- α -L-Ara4N¹⁷, but L-Ara4N is β -linked to the phosphate groups of the lipid A at 4' and 1 positions³¹, suggesting ArnT proteins are also inverting glycosyltransferases. Given these similarities with other glycan ligases, it is reasonable to find that key functional residues are located on the periplasmic exposed side of ArnT.

In this work, we demonstrate that ArnT proteins from *B. cenocepacia* and *S. enterica* share topology and functional residues. In *B. cenocepacia*, however, L-Ara4N is added to lipid A and the D-glycero-D-talo-octo-2-ulosonic acid inner core sugar, modifications that confer extremely high resistance to PmB¹³. In contrast, *S. enterica* and *E. coli* ArnT transfer L-Ara4N only to lipid A and comparatively these strains present much lower levels of PmB resistance³¹. The topological similarities and functionally conserved residues between ArnT_{Bc} and ArnT_{Se} suggest that both proteins have more in common than one would expect if they had different specificities. However, we cannot exclude the possibility that another region in ArnT_{Bc} is responsible for specific recognition of the *Burkholderia* LPS, making this protein different than that of *E. coli*, *Salmonella*, and other bacteria. Alternatively, a distinct L-Ara4N transferase could be required in *B. cenocepacia* to add L-Ara4N to the inner core D-glycero-D-talo-octo-2-ulosonic acid after ArnT transfers L-Ara4N to the lipid A. Further research is needed to investigate these possibilities and examine the sequential process of L-Ara4N incorporation to lipid A and inner core in detail.

In summary, this study provides experimental evidence that ArnT proteins from *B. cenocepacia* and *S. enterica*, which play key roles in remodeling LPS, share topological and functional similarities that also extend to other members of the ArnT family and provide insights for further investigation of ArnT proteins and the elucidation of their catalytic mechanism.

Methods

Bacterial strains and growth conditions. Bacterial strains and plasmids are listed in Supplementary Table S1 online. Growth medium was supplemented as needed with the following chemicals (final concentrations): 100 μ g ampicillin ml⁻¹, 30 μ g chloramphenicol ml⁻¹, 50 μ g trimethoprim ml⁻¹, 25 μ g gentamicin ml⁻¹, 10 μ g PmB ml⁻¹, 0.2% L-arabinose (w/v), and 0.2% L-rhamnose (w/v). Bacteria were grown aerobically at 37 °C in Luria-Bertani (LB) medium (Difco). For recombinant protein expression, bacteria were grown overnight in 5 mL of LB, diluted to A₆₀₀ of 0.1, and incubated at 37 °C for 2 h until cultures reached A₆₀₀ of 0.5, at which point L-arabinose was added and cells incubated for 3 h at 37 °C.

Construction of plasmids expressing parental and mutant ArnT proteins. A plasmid encoding ArnT_{FLAG-10xHis} was constructed by PCR amplification of a 1.7-kb fragment using *B. cenocepacia* K56-2 genomic DNA and primers 6269/6270 (Supplementary Table S2 online). The fragment was digested with *EcoRI* and *SalI* and ligated into the same sites of pXR1³⁴. This plasmid is a modified pBAD24 containing an oligonucleotide sequence encoding a FLAG plus 10x-His tag, which was placed adjacent to the multiple cloning site for construction of in-frame C-terminally FLAG-10xHis-tagged proteins. The resulting plasmid, designated pFT1, expressed ArnT_{FLAG-10xHis} under the control of the arabinose-inducible promoter. pFT1 was used as template to replace the native cysteines of ArnT (residues 154 and 176) with alanine by sequential site-direct mutagenesis using primers 6238/6239, and 6240/6241 (Supplementary Table S2 online). The plasmid encoding the cysteineless ArnT_{FLAG-10xHis} was named pFT7. For sulfhydryl labeling experiments, novel cysteines were introduced in pFT7 by PCR using primers containing the desired mutations and *Pfu* AD polymerase (Stratagene). *DpnI* was added to PCR reactions for overnight digestion of parental plasmid DNA at 37 °C. The resulting DNA was introduced into *E. coli* DH5 α by CaCl₂ transformation. Resulting plasmids were confirmed by sequencing with primers 252, 258 and 6385 (Supplementary Table S2 online).

Alkaline phosphatase (PhoA) fusions and alkaline phosphatase assay. pFT4 and pFT15, expressing FLAG-ArnT_{Bc-PhoA} and FLAG-ArnT_{Se-PhoA}, respectively, were constructed by PCR amplification of a 1.7-kb fragment from pFT1 and pMH494 with 6421/6716 and 7178/7182 primer pairs, respectively

(Supplementary Table S2 online). The amplicons were digested with *Xba*I and *Sal*I and ligated into these sites in pAH18³⁰. The ligation mixture was introduced by transformation into *E. coli* CC118 cells, and transformants plated on LB-ampicillin containing 5-bromo-4-chloro-3-indolylphosphate (60 µg ml⁻¹). Transformants were screened for blue colony phenotype denoting PhoA activity. To quantify alkaline phosphatase activity, overnight cultures were diluted 1:100 and grown for 4 h at 37 °C in LB ampicillin/0.2% arabinose, harvested, lysed, and assayed as described³⁰.

Cloning and expression of *arnT* from *S. enterica*. The *S. enterica arnT* gene was isolated by amplification of a 1.6-kb fragment using pMH494 as template and primers 6475/6476. The fragment was digested with *Eco*RI and *Sal*I and ligated into the same sites in pFT1 to replace *arnT* from *B. cenocepacia* by *S. enterica arnT*. This construct, named pFT54, expressed ArnT_{Se} with a C-terminal FLAG-10xHis tag, and was used to introduce novel cysteines by site-directed mutagenesis. For complementation of *E. coli* Δ *arnT*, alanine replacements were introduced in pFT143 (encoding *S. enterica* ArnT_{P547A}).

Topological model for ArnT. Two prediction methods were used to analyze the *in silico* topology of ArnT: PolyPhobius³⁸ and TMHMM 2.0³⁹. The ArnT models were displayed using TMRPred2D⁴⁰. Multiple-sequence alignments of ArnT homologues were performed with ClustalW (<http://www.ebi.ac.uk/clustalw/>).

Complementation of ArnT function in *B. cenocepacia*. Plasmids expressing the ArnT replacement mutant proteins were subcloned into the *Nde*I-*Hind*III site of pSCrhaB2, and the recombinant constructs introduced in the Δ *arnT-arnBC*⁺ suppressor strain by triparental mating^{41,42}. The ability of each construct to restore PmB resistance indicated ArnT function. Strains were grown overnight with 0.4% (w/v) rhamnose (to induce protein expression), diluted to 10⁻¹, 10⁻², 10⁻³, 10⁻⁴ and 10⁻⁵ and 4 µl of each dilution plated onto LB plates supplemented with 0.4% rhamnose and 10 µg ml⁻¹ PmB.

Membrane preparations and immunoblotting. Bacterial pellets were resuspended in 50 mM Tris-HCl, pH 8.0, with protease inhibitors and lysed at 10,000 PSI using a cell disruptor (Constant Systems, Kennesaw, GA). Cell debris was pelleted by centrifugation at 15,000 × *g* for 15 min at 4 °C, and the clear supernatant was centrifuged at 40,000 × *g* for 30 min at 4 °C. The pellet, containing total membranes, was suspended 50 mM Tris-HCl, pH 8.0. Protein concentration was determined by the Bradford assay (Bio-Rad). Proteins were separated by SDS-PAGE on a 12% or 18% gel (if the experiment included detection of HA-SoxY) and transferred to a nitrocellulose membrane. Immunoblots were probed with anti-FLAG and anti-HA (Sigma) mouse monoclonal antibodies. Secondary anti-mouse Alexa fluor-680 IgG antibody (Invitrogen) was used to detect fluorescence using an Odyssey infrared imaging system (LI-COR Biosciences).

Sulfhydryl labeling. Cells were cultured in 20 ml of LB broth at 37 °C from an initial OD₆₀₀ of 0.2 to an OD₆₀₀ of 0.5 at which time arabinose was added to a final concentration of 0.2% (w/v) for induction of ArnT_{FLAG-10xHis} protein expression, and growth continued for 3 h. Bacterial cells were harvested by centrifugation at 16,000 × *g* and washed with HEPES/MgCl₂ buffer (50 mM HEPES, pH 6.8; 5 mM MgCl₂). Cell pellets were resuspended in 0.3 ml of HEPES/MgCl₂ buffer and divided in three portions: 0.1 ml of cell suspension was incubated with 1 mM methoxypolyethylene glycol maleimide (PEG-Mal) at room temperature for 1 h with 50 mM EDTA for *B. cenocepacia* ArnT and 5 mM EDTA for *S. enterica* ArnT; 0.1 ml was treated with 2% SDS prior to labeling, and 0.1 ml was incubated with buffer as control. The sulfhydryl labeling reaction was stopped with 45 mM of dithiothreitol for 10 min and mixed with 3X dye buffer (50 mM Tris-HCl [pH 6.8], 2% SDS, 10% glycerol, and 0.1% bromophenol blue), and incubated for 30 min at 45 °C. Mild denaturation conditions were used to optimize ArnT detection, as these conditions work best for membrane proteins⁴³. The crude membrane fraction was resuspended in 50 µl of HEPES/ MgCl₂ buffer supplemented with protease inhibitors. 25 µl were labeled with 1 mM PEG-Mal at room temperature for 1 h. The reaction was quenched by adding 45 mM of dithiothreitol for 10 min, and centrifuged at 16,000 × *g* for 1 min. Pellets were suspended in 50 µl of HEPES/MgCl₂ buffer with protease inhibitor. Control samples were incubated with buffer alone. Protein was extracted and processed as described above.

Thiol-specific chemical blocking with N-ethylmaleimide (NEM). Cell suspensions in HEPES/MgCl₂ buffer (0.1 ml) were incubated with 5 mM N-ethylmaleimide (NEM) for 30 min at room temperature, and centrifuged at 16,000 × *g* for 1 min. Pellets were washed twice with 1 ml of iced HEPES/MgCl₂ buffer. The samples were suspended in 200 µl of HEPES/MgCl₂ buffer, and incubated with 2% SDS and 1 mM PEG-Mal for 1 h at room temperature. Samples were quenched with 45 mM of dithiothreitol for 10 min. Protein extraction was performed as described above.

MIC determination. The MIC was determined on solid media using PmB E-test strips. Overnight cultures, were diluted to an A₆₀₀ of 0.004 in sterile PBS and used to streak LB agar plates using a sterile cotton swab. E-test strips containing PmB were added and plates were incubated for 24 h at 37 °C. MIC was defined as the lowest concentration of PmB to show growth inhibition.

Lipid A isolation and mass spectrometry. L-Ara4N modifications of lipid A were identified by mass spectrometry (MS) using matrix-assisted laser desorption/ionization-time of flight (MALDI-TOF). Cells were grown overnight in LB medium (100 ml) supplemented with 50- $\mu\text{g ml}^{-1}$ trimethoprim and 0.4% rhamnose. Cultures were centrifuged (10,000 $\times g$), washed twice with phosphate buffer (10 mM Na_2HPO_4 , 1.7 mM KH_2PO_4) and freeze-dried. Lipid A was extracted from lyophilized cells and desalted, as previously described⁴⁴. For MS analysis, dihydroxybenzoic acid (DHB) (Sigma Chemical Co., St. Louis, MO) was used as a matrix and prepared to saturation in acetonitrile: 0.1% trifluoroacetic acid (1:2 v/v). Two-microliters of sample was loaded on the target, dried, and covered by 1 μl of DHB. The target was inserted in a Bruker Autoflex MALDI-TOF spectrometer. Data acquisition and analysis were performed using the Flex Analysis software.

References

- Govan, J. R. & Deretic, V. Microbial pathogenesis in cystic fibrosis: mucoid *Pseudomonas aeruginosa* and *Burkholderia cepacia*. *Microbiol Rev* **60**, 539–574 (1996).
- Fang, K. *et al.* Exploring the metabolic network of the epidemic pathogen *Burkholderia cenocepacia* J2315 via genome-scale reconstruction. *BMC Syst Biol* **5**, 83 (2011).
- Leitão, J. H. *et al.* Variation of the antimicrobial susceptibility profiles of *Burkholderia cepacia* complex clonal isolates obtained from chronically infected cystic fibrosis patients: a five-year survey in the major Portuguese treatment center. *Eur J Clin Microbiol Infect Dis* **27**, 1101–1111 (2008).
- Loutet, S. A. & Valvano, M. A. Extreme antimicrobial peptide and polymyxin B resistance in the genus *Burkholderia*. *Front Cell Infect Microbiol* **1**, 6 (2011).
- Loutet, S. A., Di Lorenzo, F., Clarke, C., Molinaro, A. & Valvano, M. A. Transcriptional responses of *Burkholderia cenocepacia* to polymyxin B in isogenic strains with diverse polymyxin B resistance phenotypes. *BMC Genomics* **12**, 472 (2011).
- Ortega, X., Silipo, A., Saldías, M. S., Bates, C. C., Molinaro, A. & Valvano, M. A. Biosynthesis and structure of the *Burkholderia cenocepacia* K56-2 lipopolysaccharide core oligosaccharide: truncation of the core oligosaccharide leads to increased binding and sensitivity to polymyxin B. *J Biol Chem* **284**, 21738–21751 (2009).
- Loutet, S. A., Mussen, L. E., Flannagan, R. S. & Valvano, M. A. A two-tier model of polymyxin B resistance in *Burkholderia cenocepacia*. *Environ Microbiol Rep* **3**, 278–285 (2011).
- Loutet, S. A., Flannagan, R. S., Kooi, C., Sokol, P. A. & Valvano, M. A. A complete lipopolysaccharide inner core oligosaccharide is required for resistance of *Burkholderia cenocepacia* to antimicrobial peptides and bacterial survival *in vivo*. *J Bacteriol* **188**, 2073–2080 (2006).
- Silipo, A. *et al.* The complete structure and pro-inflammatory activity of the lipooligosaccharide of the highly epidemic and virulent gram-negative bacterium *Burkholderia cenocepacia* ET-12 (strain J2315). *Chemistry* **13**, 3501–3511 (2007).
- Ortega, X., Silipo, A., Saldías, M. S., Bates, C. C., Molinaro, A. & Valvano, M. A. Biosynthesis and structure of the *Burkholderia cenocepacia* K56-2 lipopolysaccharide core oligosaccharide: truncation of the core oligosaccharide leads to increased binding and sensitivity to polymyxin B. *J Biol Chem* **284**, 21738–21751 (2009).
- Vinion-Dubiel, A. D. & Goldberg, J. B. Lipopolysaccharide of *Burkholderia cepacia* complex. *J Endotoxin Res* **9**, 201–213 (2003).
- Ortega, X. P. *et al.* A putative gene cluster for aminoarabinose biosynthesis is essential for *Burkholderia cenocepacia* viability. *J Bacteriol* **189**, 3639–3644 (2007).
- Hamad, M. A., Di Lorenzo, F., Molinaro, A. & Valvano, M. A. Aminoarabinose is essential for lipopolysaccharide export and intrinsic antimicrobial peptide resistance in *Burkholderia cenocepacia*. *Mol Microbiol* **85**, 962–974 (2012).
- El-Halfawy, O. M. & Valvano, M. A. Chemical communication of antibiotic resistance by a highly resistant subpopulation of bacterial cells. *PLoS One* **8**, e68874 (2013).
- Raetz, C. R., Reynolds, C. M., Trent, M. S. & Bishop, R. E. Lipid A modification systems in gram-negative bacteria. *Annu Rev Biochem* **76**, 295–329 (2007).
- Yan, A., Guan, Z. & Raetz, C. R. An undecaprenyl phosphate-aminoarabinose flippase required for polymyxin resistance in *Escherichia coli*. *J Biol Chem* **282**, 36077–36089 (2007).
- Trent, M. S., Ribeiro, A. A., Lin, S., Cotter, R. J. & Raetz, C. R. An inner membrane enzyme in *Salmonella* and *Escherichia coli* that transfers 4-amino-4-deoxy-L-arabinose to lipid A: induction on polymyxin-resistant mutants and role of a novel lipid-linked donor. *J Biol Chem* **276**, 43122–43131 (2001).
- Miller, S. I., Ernst, R. K. & Bader, M. W. LPS, TLR4 and infectious disease diversity. *Nat Rev Microbiol* **3**, 36–46 (2005).
- Raetz, C. R. & Whitfield, C. Lipopolysaccharide endotoxins. *Annu Rev Biochem* **71**, 635–700 (2002).
- Wang, X., Ribeiro, A. A., Guan, Z. & Raetz, C. R. Identification of undecaprenyl phosphate-beta-D-galactosamine in *Francisella novicida* and its function in lipid A modification. *Biochemistry* **48**, 1162–1172 (2009).
- Marr, N., Tirsoaga, A., Blanot, D., Fernandez, R. & Caroff, M. Glucosamine found as a substituent of both phosphate groups in *Bordetella* lipid A backbones: role of a BvgAS-activated ArnT ortholog. *J Bacteriol* **190**, 4281–4290 (2008).
- Rolin, O. *et al.* Enzymatic modification of lipid A by ArnT protects *Bordetella bronchiseptica* against cationic peptides and is required for transmission. *Infect Immun* **82**, 491–499 (2014).
- Impellitteri, N. A., Merten, J. A., Bretscher, L. E. & Klug, C. S. Identification of a functionally important loop in *Salmonella typhimurium* ArnT. *Biochemistry* **49**, 29–35 (2010).
- Koch, S., Fritsch, M. J., Buchanan, G. & Palmer, T. *Escherichia coli* TatA and TatB proteins have N-out, C-in topology in intact cells. *J Biol Chem* **287**, 14420–14431 (2012).
- Nasie, I., Steiner-Mordoch, S. & Schuldiner, S. Topology determination of untagged membrane proteins. *Methods Mol Biol* **1033**, 121–130 (2013).
- Bogdanov, M., Zhang, W., Xie, J. & Dowhan, W. Transmembrane protein topology mapping by the substituted cysteine accessibility method (SCAM(TM)): application to lipid-specific membrane protein topogenesis. *Methods* **36**, 148–171 (2005).
- Rivera-Ordaz, A. *et al.* The sodium/proline transporter PutP of *Helicobacter pylori*. *PLoS One* **8**, e83576 (2013).
- Kuper, C. & Jung, K. CadC-mediated activation of the cadBA promoter in *Escherichia coli*. *J Mol Microbiol Biotechnol* **10**, 26–39 (2005).
- Haardt, M. & Bremer, E. Use of phoA and lacZ fusions to study the membrane topology of ProW, a component of the osmoregulated ProU transport system of *Escherichia coli*. *J Bacteriol* **178**, 5370–5381 (1996).
- Marolda, C. L. *et al.* Membrane topology and identification of critical amino acid residues in the Wzx O-antigen translocase from *Escherichia coli* O157:H4. *J Bacteriol* **192**, 6160–6171 (2010).
- Silipo, A. *et al.* Complete structural characterization of the lipid A fraction of a clinical strain of *B. cepacia* genomovar I lipopolysaccharide. *Glycobiology* **15**, 561–570 (2005).

32. Bretscher, L. E., Morrell, M. T., Funk, A. L. & Klug, C. S. Purification and characterization of the L-Ara4N transferase protein ArnT from *Salmonella typhimurium*. *Protein Expr Purif* **46**, 33–39 (2006).
33. Needham, B. D. & Trent, M. S. Fortifying the barrier: the impact of lipid A remodelling on bacterial pathogenesis. *Nat Rev Microbiol* **11**, 467–481 (2013).
34. Ruan, X., Loyola, D. E., Marolda, C. L., Perez-Donoso, J. M. & Valvano, M. A. The WaaL O-antigen lipopolysaccharide ligase has features in common with metal ion-independent inverting glycosyltransferases. *Glycobiology* **22**, 288–299 (2012).
35. Korres, H. & Verma, N. K. Topological analysis of glucosyltransferase GtrV of *Shigella flexneri* by a dual reporter system and identification of a unique reentrant loop. *J Biol Chem* **279**, 22469–22476 (2004).
36. Korres, H. & Verma, N. K. Identification of essential loops and residues of glucosyltransferase V (GtrV) of *Shigella flexneri*. *Mol Membr Biol* **23**, 407–419 (2006).
37. Nikaido, K. & Nikaido, H. Glucosylation of lipopolysaccharide in *Salmonella*: biosynthesis of O antigen factor n12. II. Structure of the lipid intermediate. *J Biol Chem* **246**, 3912–3919 (1971).
38. Käll, L., Krogh, A. & Sonnhammer, E. L. An HMM posterior decoder for sequence feature prediction that includes homology information. *Bioinformatics* **21** (Suppl 1), i251–257 (2005).
39. Sonnhammer, E. L., von Heijne, G. & Krogh, A. A hidden Markov model for predicting transmembrane helices in protein sequences. *Proc Int Conf Intell Syst Mol Biol* **6**, 175–182 (1998).
40. Spyropoulos, I. C., Liakopoulos, T. D., Bagos, P. G. & Hamodrakas, S. J. TMRPres2D: high quality visual representation of transmembrane protein models. *Bioinformatics* **20**, 3258–3260 (2004).
41. Craig, F. F., Coote, J. G., Parton, R., Freer, J. H. & Gilmour, N. J. A plasmid which can be transferred between *Escherichia coli* and *Pasteurella haemolytica* by electroporation and conjugation. *J Gen Microbiol* **135**, 2885–2890 (1989).
42. Figurski, D. H. & Helinski, D. R. Replication of an origin-containing derivative of plasmid RK2 dependent on a plasmid function provided in trans. *Proc Natl Acad Sci U S A* **76**, 1648–1652 (1979).
43. Ruan, X. & Valvano, M. A. *In vitro* O-antigen ligase assay. *Methods Mol Biol* **1022**, 185–197 (2013).
44. El Hamidi, A., Tirsoaga, A., Novikov, A., Hussein, A. & Caroff, M. Microextraction of bacterial lipid A: easy and rapid method for mass spectrometric characterization. *J Lipid Res* **46**, 1773–1778 (2005).

Acknowledgements

This work was supported grants from the Canadian Institutes of Health Research, the UK Cystic Fibrosis Trust (to M.A.V.), and COST action BM1003 “Microbial cell surface determinants of virulence as targets for new therapeutics in cystic fibrosis”. We thank Dr. M. Hamad for technical assistance, Dr. C. Klug for the gift of *E. coli* BL21(DE3) Δ arnT, and Dr. J. Bengoechea for assistance with MALDI-TOF spectrometry.

Author Contributions

F.T.-C. and M.A.V. designed all the research, analyzed the data and wrote the manuscript. F.T.-C. performed the experiments. K.B.P. performed and analyzed mass spectrometry data. All authors reviewed and approved the manuscript.

Additional Information

Supplementary information accompanies this paper at <http://www.nature.com/srep>

Competing financial interests: The authors declare no competing financial interests.

How to cite this article: Tavares-Carreón, F. *et al.* Burkholderia cenocepacia and Salmonella enterica ArnT proteins that transfer 4-amino-4-deoxy-L-arabinose to lipopolysaccharide share membrane topology and functional amino acids. *Sci. Rep.* **5**, 10773; doi: 10.1038/srep10773 (2015).



This work is licensed under a Creative Commons Attribution 4.0 International License. The images or other third party material in this article are included in the article's Creative Commons license, unless indicated otherwise in the credit line; if the material is not included under the Creative Commons license, users will need to obtain permission from the license holder to reproduce the material. To view a copy of this license, visit <http://creativecommons.org/licenses/by/4.0/>